Finite Dimensional Approximation to Muscular Response in Force-Fatigue Dynamics using Functional Electrical Stimulation

Toufik Bakir, Bernard Bonnard, Sandrine Gayrard, Jérémy Rouot

Finite Dimensional Approximation to Muscular Response in Force-Fatigue Dynamics using Functional Electrical Stimulation

Toufik Bakir [a], Bernard Bonnard [b], Sandrine Gayrard [a,b], Jérémy Rouot [c]

[a] *Univ. Bourgogne Franche-Comté, ImViA Laboratory EA 7508, 9 avenue Alain Savary, Dijon, France*

[b] *INRIA, 2004 Route des Lucioles, 06902 Valbonne, France*

[c] *L@bisen, Vision-AD Team, Yncrea Ouest, 20 Rue Cuirassé Bretagne, Brest, France*

Abstract

Recent dynamical models, based on the seminal work of V. Hill, allow to predict the muscular response to functional electrostimulation (FES), in the isometric and non-isometric cases. The physical controls are modeled as Dirac pulses and lead to a sampled-data control system, sampling corresponding to times of the stimulation, where the output is the muscular force response. Such a dynamics is suitable to compute optimized controls aiming to produce a constant force or force strengthening, but is complex for real time applications. The objective of this article is to construct a finite dimensional approximation of this response to provide fast optimizing schemes, in particular for the design of a smart electrostimulator for muscular reinforcement or rehabilitation. It is an on-going industrial project based on force-fatigue models, validated by experiments. Moreover it opens the road to application of optimal control to track a reference trajectory in the joint angular variable to produce movement in the non-isometric models.

Key words: Biomechanics · Force-fatigue models · Sampled-data control problem · Nonlinear input-output approximation · Predictive-correction methods in optimization.

1 Introduction

Based on the seminal work of V. Hill [10], recent mathematical models (validated by experiments) allow to predict the force response to external stimulation. They are presented and discussed in details in [19] in the non-fatigue isometric case. They were extended in particular by Ding et al. [7–9] to take into account the muscular fatigue due to a long stimulation period and later in [14] to analyze the joint angular variable response, in the non-isometric case aiming to produce movements. Such models contain two basic nonlinearities to model the complexity of the dynamics. Fist of all, the ionic conduction and the nonlinear effect of successive pulses on the Ca^{2+}-concentration. Second, the nonlinear dynamics relating the muscular force response to such concentration, modeled by the Michaelis-Menten-Hill functions [15].

For each train of pulses, due to digital constraints, only a finite number of pulses can be applied and from the optimal control point of view, the problem fits into the frame of optimal sampled-data control problems, studied in particular in [4] to derive Pontryagin necessary conditions. They can be analyzed to determine optimized train pulses

⋆ This paper was not presented at any IFAC meeting. It benefited from the support of the FMJH Program PGMO and from the support of EDF; Thales, Orange and the authors are partially supported by the Latex AMIES. Corresponding author J. Rouot. Email. jeremy.rouot@yncrea.fr.

Email addresses: toufik.bakir@u-bourgogne.fr (Toufik Bakir), bernard.bonnard@u-bourgogne.fr (Bernard Bonnard), sandrine.gayrard@grenoble-inp.org (Sandrine Gayrard), jeremy.rouot@yncrea.fr (Jérémy Rouot).

and compared with direct optimizing schemes. A previous series of articles described the optimal control problems related to track a reference force or force strengthening, the control being either the interpulse $I_i = t_i - t_{i-1}$ between two successive pulses or the amplitude of each pulse. In particular, model predictive control (MPC) method is presented in [1] aiming the use of online optimized closed loop control in the applications using force-fatigue model, as suggested in [6]. Direct methods vs indirect methods based on Pontryagin type necessary conditions are discussed and numerically implemented in [2] for the isometric case or in [3] for the non-isometric case.

The conclusion of aforementioned articles is that the nonlinear dynamics is computationally expensive in the numerical integration procedure and a challenging task is to reduce this time for real time computation in the applications. This article is motivated by the design of a smart electrostimulator, where the Ding et al. model is used to adjust automatically the frequency and the amplitude of the stimulations and to compute the sequence of stimulations and rest periods adapted to the task of the training program, e.g. endurance program or force strengthening program. The objective of this article being to bypass the computational difficulty by constructing a finite dimensional approximation of the force response, depending upon the parameters of each individual, which can be online estimated, aiming a real time computation of the optimized amplitudes and times, for each training program. Note that this approximation has been coded and the application scheme to the smart electrostimulator is briefly presented in the final section.

The article is organized as follows. In section 2, the mathematical model called the Ding et al. model [7–9] is presented and the main properties of the dynamics are described, reflecting the features of the muscular activity. Hence our analysis can be applied to different models discussed in [19]. The section 3 presents the optimization problems, in relation with muscular dynamics and oriented towards the design of a smart electrostimulator, where each training program must be translated into an optimization problem. Section 4 is the technical contribution of this article, that is the construction of the approximation for real time computation. In section 5, we present some numerical simulations aiming to validate the approximation and the optimizing scheme. In the final section 6, we outline the application to the design of the smart electrostimulator. It is based on a nonlinear output tracking [11–13] as a general theoretical frame and is applied to produce a constant force in our situation, but it can be extended to the non-isometric case to obtain any reference force. The conclusion indicates directions to complete our analysis, related to online parameters estimation of the problems [17,19] and MPC-methods [16,18] suitable for practical applications.

2 Mathematical model and main properties

We present the Ding et al. model force-fatigue model [7–9], extension of the original Hill model [10].

2.1 Ding et al. force-fatigue model [7–9]

The FES input u over a pulse train $[0, T]$ is given by

$$u(t) = \sum_{i=0}^{n} \eta_i \delta(t - t_i), \quad t \in [0, T], \tag{1}$$

where $0 = t_0 < t_1 < \cdots < t_n < T$ are the impulsion times with $n \in \mathbb{N}$ being fixed and η_i being the amplitudes of each pulses, which are convexified by taking $\eta_i \in [0, 1]$, $\delta(t - t_i)$ denoting the Dirac function at time t_i.

Such physical control will provide the FES-signal denoted by $E(t)$, which drives the force response using electrical conduction and its dynamics is given by

$$\dot{E}(t) + \frac{E(t)}{\tau_c} = \frac{1}{\tau_c} \sum_{i=0}^{n} R_i \eta_i \delta(t - t_i), \ a.e.\ t \in [0, T], \tag{2}$$

with $E(0) = 0$, depending upon the time response τ_c and the scaling function R_i defined by

$$R_i = \begin{cases} 1 & \text{if } i = 0 \\ 1 + (\bar{R} - 1)\, e^{-(t_i - t_{i-1})/\tau_c} & \text{otherwise} , \end{cases}$$

which codes the memory effect of successive muscle contractions and is associated to *tetanus* [19].

The first result is:

Lemma 1 *Integrating* (2)*, one gets*

$$E(t) = \frac{1}{\tau_c} \sum_{i=0}^{n} R_i e^{-\frac{t-t_i}{\tau_c}} \eta_i H(t-t_i),$$

where H is the Heaviside function and the FES signal depends upon two parameters $(\tau_c, \bar{R})$.

Definition 2 *Consider a control system of the form: $\frac{\mathrm{d}x}{\mathrm{d}t} = f(x,u)$ where $x \in \mathbb{R}^n$, $u \in U \subset \mathbb{R}^m$. It is said permanent if u is a measurable bounded mapping valued in U. It is called a sampled-data control system if the set of controls is restricted to the set of piecewise constant mappings $[u_0, u_1, \ldots, u_n]$, $u_i \in U$ over a set of times $t_0 = 0 < t_1 < \cdots < t_n < T$, where n is a fixed integer.*

Our problem can be formulated in the sampled-data control frame. One can write from (1),

$$E(t) = \frac{e^{-t/\tau_c}}{\tau_c} \sum_{i=0}^{n} R_i \eta_i e^{-t_i/\tau_c} H(t-t_i) = \sum_{i=0}^{n} u_i(t),$$

where $u_i(t)$ is the effect of the pulse $\eta_i \delta(t-t_i)$ on the linear dynamics (2). One introduces the following.

Definition 3 *For each i in $\{0, \ldots, n\}$, the restriction of u_i to $[t_i, t_{i+1}]$ is called the head and the restriction to $[t_{i+1}, T]$ is called the tail.*

Clearly the FES-input is in the generalized frame of sampled data control system, provided we take into account the time-dependence and the phenomenon of tetanus. Observe also that each impulse have an effect on the whole train $[0, T]$.

The FES signal drives the evolution of the electrical conduction according to the linear dynamics describing the evolution of Ca^{2+}-concentration c_N:

$$\dot{c}_N(t) + \frac{c_N(t)}{\tau_c} = E(t) \tag{3}$$

and integrating the (resonant) system with $c_N(0) = 0$ yields the following:

Proposition 4 *The concentration is*

$$c_N(t) = \frac{1}{\tau_c} \sum_{i=0}^{n} R_i \eta_i (t-t_i)\, e^{-\frac{t-t_i}{\tau_c}} H(t-t_i), \tag{4}$$

which are the superposition of lobes of the form

$$\ell_i(t) = \frac{1}{\tau_c} R_i \eta_i (t-t_i)\, e^{-\frac{t-t_i}{\tau_c}}, \tag{5}$$

whose restriction to $[t_i, t_{i+1}]$ forms the head of the corresponding lobe.

PROOF. Apply a time translation to the initial lobe with $R_0 = 1$.

Introducing the functions

$$m_1(t) = \frac{c_N(t)}{K_m + c_N(t)}, \quad m_2(t) = \frac{1}{\tau_1 + \tau_2\, m_1(t)}, \tag{6}$$

where m_1 is the *Michaelis-Menten-Hill function* [15], the force response satisfies the Hill dynamics

$$\dot{F}(t) = -m_2(t)\, F(t) + m_1(t)A, \tag{7}$$

and where A, K_m, τ_1, τ_2 being additional parameters and we denote by $\Lambda = (\bar{R}, \tau_c, A, K_m, \tau_1, \tau_2)$ the whole set of parameters.
The model can be extended to take into account the fatigue. Using sensitivity analysis from [3], we shall restrict our study to the case of the *force-fatigue Ding et al. model* with the single equation:

$$\dot{A}(t) = -\frac{A(t) - A_{rest}}{\tau_{fat}} + \alpha_A\, F(t) \tag{8}$$

for all $t \in [0, t_f]$, where t_f is the total time and $A(0) = A_{rest}$ corresponds to the fixed value of A for the non fatigue model. This leads to introduce additional parameters τ_{fat}, α_A. Typical parameters values used in this article to validate numeric simulations are reported in Table 1 .

2.2 Mathematical rewriting

For the previous force-fatigue model and for the sake of the analysis, the model is rewritten as the control system:

$$\dot{x}(t) = g(x(t)) + b(t) \sum_{i=0}^{n} G(t_{i-1}, t_i)\eta_i\, H(t - t_i)\, \boldsymbol{e}$$

with $x = (x_1, \ldots, x_8)^\intercal = (c_N, F, A, \bar{R}, \tau_c, \tau_1, \tau_2, K_m)^\intercal$ which splits into state variables (c_N, F, A) and fatigue parameters $\Lambda = (\bar{R}, \tau_c, \tau_1, \tau_2, K_m)$ satisfying the dynamics $\dot{\Lambda}(t) = 0$, the system being integrated with the initial condition $x_0 = (0, 0, A_{rest}, \Lambda(0))^\intercal$ and

$$\begin{aligned} &\boldsymbol{e} = (1, 0 \ldots, 0)^\intercal, && b(t) = \tfrac{1}{\tau_c} e^{-t/\tau_c}, \\ &G(t_{i-1}, t_i) = (\bar{R} - 1)e^{t_{i-1}/\tau_c} + e^{t_i/\tau_c}, \end{aligned}$$

where $t_{-1} = -\infty, t_0 = 0$ and $t_{n+1} = T$.

This leads to a control system of the form

$$\dot{x}(t) = g(x(t)) + b(t) \sum_{i=0}^{n} G(t_{i-1}, t_i)\eta_i H(t - t_i)\ \boldsymbol{e}$$

with $x(0) = x_0$.

The variable $\sigma = (t_1, \ldots, t_n, \eta_0, \eta_1, \ldots, \eta_n)$ denotes the finite dimensional input-space with the constraints

$$\begin{aligned} &\eta_i \in [0, 1],\ i = 0, \ldots, n \\ &0 < t_1 < \cdots < t_n < T, \quad t_i - t_{i-1} \geq I_{\min}, \quad i = 1, \ldots, n\ , \end{aligned}$$

where $I_{\min}$ is the smallest admissible interpulse.

Moreover the control is observed using the following observation function

$$y(t) = h(x(t)), \tag{9}$$

and $h : x \mapsto (F, A)$ serves as a direct measure of the muscular force and the fatigue variable.

The following properties are straightforward but crucial in our analysis.

Proposition 5 *The input-output mapping $\sigma \mapsto y(t)$ is piecewise smooth over $[0,T]$ and smooth if $t \neq t_i,\ i = 0,\dots,n$ (impulse times).*

Proposition 6 *For the non fatigue model, the force response can be integrated up to a time reparameterization as*

$$F(s) = \int_0^s e^{u-s} m_3(u)\,\mathrm{d}u \tag{10}$$

with

$$m_3(s) = A\frac{m_1(s)}{m_2(s)}, \quad \mathrm{d}s = m_2(t)\,\mathrm{d}t. \tag{11}$$

PROOF. Hill dynamics (7) is rewritten as

$$\frac{\mathrm{d}F}{\mathrm{d}s} = m_3(s) - F(s)$$

and this linear dynamics can be integrated using Lagrange formula with $F(0) = 0$. This proves the assertion. □

3 Optimization problems related to the design of the electrostimulator

3.1 Standard electrostimulators vs smart electrostimulators

The standard commercial electrostimulators apply a sequence of pulses trains and rest periods, where on each train $[0,T]$ the user only imposes the amplitude of the pulses trains and the constant frequency is related to training program, typically low frequency for endurance program and high frequency for force strengthening program. Our aim is to introduce optimization problems related to the design of a smart electrostimulator, which will be discussed in Section 6.

3.2 Optimization problems

3.2.1 The punch program

In this case, our aim is to optimize the force at the end of the train over each train $[0,T]$. This leads to:

OCP1: $\max_\sigma F(T)$.
In this case, the amplitudes can be held at the constant maximal values $\eta_i = 1,\ i = 0,\dots,n$ and the optimization variables are the impulse times:

$$0 = t_0 < t_1 < \cdots < t_n < T.$$

Since one considers a single train, the force model is sufficient.

3.2.2 The train endurance program

We consider a single train $[0,T]$ on which the model is the force model and the corresponding problem is

OCP2: $\min_\sigma \int_0^T |F(t) - F_{ref}|^2\,\mathrm{d}t$.
Here, the amplitudes are appended to the impulse times to form the optimization variables and we use the convexified amplitudes constraints: $\eta_i \in [0,1],\ i = 0,\dots,n$.

The force reference has to be adjusted in relation with the user and can be set to $F_{\max}/k$, where k is a suitable positive number greater than 1 and $F_{\max}$ is deduced from **OCP1**.

3.2.3 The endurance program

We consider an interval $[0, t_f]$, where t_f is the total training period formed by sequences of stimulation and rest periods. In this case, one must use a force-fatigue model and we take into account the constraint $A \in [A_{rest}, A_{rest}/k'']$, where $S = A_{rest}/k''$ corresponds to a *fatigue threshold* since, as reported in [7], if the user is exhausted, the force signal is *totally noisy*. Moreover in the case of exhaustion, a large rest period is required. This constraint can be penalized as follows

OCP3: $\min_\sigma \int_0^{t_f} |F(t) - F_{ref}|^2 \,\mathrm{d}t \, + \, w_1 \int_0^{t_f} |A(t) - A_S|^2 \,\mathrm{d}t,$
where A_S is related to S, while w_1 is a weight parameter.

4 Construction of an integrable model for real time application

4.1 Mathematical analysis of c_N

A pulses train is defined by a finite sequence of impulse times $\sigma = (t_i)_{0 \le i \le n}$ such that $t_0 < \cdots < t_n$ and we extend it to the left by $t_{-1} = -\infty$ and to the right by $t_{n+1} = T$. The response c_N can be decomposed as a sum of lobes defined as follows.

Definition 7 *A lobe at t_k is the representative curve of the function $\ell_k : \mathbb{R} \ni t \mapsto R_k \eta_k \, \frac{t - t_k}{\tau_c} \, e^{-(t-t_k)/\tau_c} \, H(t - t_k)$.*

Property 8 • *A lobe at t_k reaches its maximum at $t = t_k + \tau_c$ and is equal to $R_k\eta_k/e$. It is strictly increasing on $[t_k, t_k + \tau_c]$ and strictly decreasing $[t_k + \tau_c, t_{k+1}]$.*
• *ℓ_k has a unique zero at $t_k + 2\tau_c$ and therefore, ℓ_k is concave on $[t_k, t_k + 2\tau_c]$ and convex on $[t_k + 2\tau_c, t_{k+1}]$.*
• *ℓ defines a density probability function and more than 95% of the values lie in $[t_k, t_k + 5\tau_c]$. For all $t \ge t_k + 5\tau_c$, $|\ell_k(t)| \le R_k\eta_k \, 5e^{-5}$.*

Proposition 9 *Denote for $k = 0, \ldots, n$, $c_N^k = c_{N_{|[t_k, t_{k+1}]}}$ and $\bar{c}_N^k = \dfrac{1}{t_{k+1} - t_k} \int_{t_k}^{t_{k+1}} c_N(t) \,\mathrm{d}t$. We have*

$$\begin{aligned} c_N^k &= \sum_{i=0}^{k} R_i \eta_i \frac{t - t_i}{\tau_c} e^{-(t-t_i)/\tau_c}, \\ \bar{c}_N^k &= \frac{1}{t_{k+1} - t_k} \sum_{i=0}^{k} R_i \eta_i \left(\chi_i(t_k) - \chi_i(t_{k+1}) \right), \end{aligned} \tag{12}$$

where $\chi_i(t) = e^{-(t-t_i)/\tau_c} \, (\tau_c + t - t_i)$.

Definition 10 *The polynomial-exponential category for (piecewise) smooth functions $[0, T] \mapsto \mathbb{R}$ is the category generated by sums, products of polynomials $P(t)$ and exponential mappings to generate exponential-polynomials: $\sum_n P_n(t) e^{\lambda_n t}$. This category is stable with respect to derivation and integration.*

Using proposition 4 one has:

Lemma 11 *For $t \neq t_i$, $c_N(t)$ is in the polynomial-exponential category. Moreover, the coefficients are linear with respect to η_i and polynomial-exponential with respect to t_i.*

We introduce the notion of p-persistent pulses related to the case where pth successive lobes have an influence on the $(p+1)$th lobe.

Definition 12 *Let $t_1 < \cdots < t_p$ be p successive impulses times of a pulses train satisfying for any $i \in [\![1, p]\!]$, $t_i \le t_{i-1} + 5$ and $t_i - t_{i-1} \ge I_{\min}$. When such integer p is maximal then the pulses train is said p-persistent.*

Remark 13 *Given an 1-persistent pulses train $(t_i)_{1\le i\le n}$ $(n>1)$, there exists $j\in[\![1,n]\!]$ such that $t_j > t_{j-1}+5$. Then, by Property 8, c_N^j is well approximated by $t\mapsto (t-t_j)\,e^{-(t-t_j)}$ for $t\in[t_j,t_{j+1}]$ (the factor $R_j^\dagger$ has a negligible effect).*

We define now an approximation of c_N denoted as $\tilde{c}_N$ that will be used to construct an approximation of the force F limiting the number of terms and the error between c_N and $\tilde{c}_N$ is analyzed in the following proposition.

Proposition 14 *Let $(t_i)_{1\le i\le n}$ be a p-persistent pulses train. Denote*

$$c_N(t) \coloneqq \sum_{i=0}^{k} R_i^\dagger \eta_i (t-t_i)\, e^{-(t-t_i)}$$

and define its (lower) approximation by

$$\tilde{c}_N(t) \coloneqq \sum_{i=\max(0,k-p+1)}^{k} R_i^\dagger \eta_i (t-t_i)\, e^{-(t-t_i)}$$

for $t\in[t_k,t_{k+1}]$, $k=0,\dots,n$.
Then, we have:

$$\sup_{t\in[t_k,t_{k+1}]} c_N(t)-\tilde{c}_N(t) \le \frac{\bar{R}}{e}\,\kappa + 5e^{-5}\bar{R}(k-p-\kappa+1),$$

where $\lceil\cdot\rceil$ is the ceiling function and $\kappa=\min\left(p,\left\lceil\frac{5\tau_c}{I_{\min}}\right\rceil\right)$ is independent of k.

PROOF. For $t\in[t_k,t_{k+1}]$, $k=0,\dots,n$, we have:

$$c_N(t) \ge \sum_{i=k-p+1}^{k} R_i^\dagger \eta_i (t-t_i) e^{-(t-t_i)} = \tilde{c}_N(t)$$

and

$$c_N(t)-\tilde{c}_N(t) \le \bar{R}\sum_{i=0}^{k-p}(t-t_i)e^{-(t-t_i)}.$$

The number of indices $i\in\{0,\dots,k-2\}$ for which $t-t_i\le 5\tau_c$ is at most $\kappa\coloneqq\min\left(p,\left\lceil\frac{5\tau_c}{I_{\min}}\right\rceil\right)$ since $(t_i)_i$ is p-persistent and $\left\lceil\frac{5\tau_c}{I_{\min}}\right\rceil$ stands for the maximum number of impulse times satisfying the constraint $t_i-t_{i-1}\ge I_{\min}$ in an interval of length $5\tau_c$.

Proposition 15 (Tail approximation of c_N) *Let $q\in\{0,\dots,n\}$. Denote the tail of c_N by $c_N^q = c_{N|_{[t_q,T]}}$ and its average over $[t_q,T]$ by $\bar{c}_N^q$. We have:*

$$\bar{c}_N^q = \frac{1}{T-t_q}\sum_{i=0}^{q} R_i\eta_i\left(\chi_i(t_q)-\chi_i(T)\right) + \frac{1}{T-t_q}\sum_{i=q+1}^{n} R_i\eta_i\left(1-\chi_i(T)\right), \tag{13}$$

where $\chi_i(t)=e^{-(t-t_i)}\,(1+t-t_i)$.

4.2 Approximations of F

Integrating (7), the force with $F(0)=0$ can be written as

$$F(t) = AM(t)\int_0^t M^{-1}(s)m_1(s)\,\mathrm{d}s,\ t\in[0,T] \tag{14}$$

where $M(t) = \exp\left(-\int_0^t m_2(s)\,\mathrm{d}s\right)$.

The following properties show that it is natural to approximate m_1 and m_2 by polynomial functions.

Property 16 *Let $k \in \{0,\dots,n\}$.*

- *Denote $t^* = \underset{t\in[t_k,t_{k+1}]}{\operatorname{argmax}}\ c_N(t)$. Then, m_1 (resp. m_2) is strictly increasing (resp. decreasing) on $[t_k, t^*]$ and strictly decreasing (resp. increasing) of $[t^*, t_{k+1}]$.*
- *If $t_{k+1} < t_k + 2\tau_c$ then $m_{1|[t_k,t_{k+1}]}$ is concave and $m_{2|[t_k,t_{k+1}]}$ is convex.*

We consider a finer partition of $(t_i)_{1\le i\le n}$ denoted as $(t_{i+j/p})_{0\le i\le n,\,0\le j\le p-1}$, $p \in \mathbb{N}^*$, such that it satisfies $t_i < t_{i+1/p} < \cdots < t_{i+(p-1)/p} < t_{i+1}$. We approximate m_1 and m_2 on each interval $[t_{i+j/p}, t_{i+(j+1)/p}]$ by a polynomial function denoted respectively by $\tilde{m}_1$ and $\tilde{m}_2$.

Example 17 (Triangular approximation of a lobe.) *Since $\dot{m}_1 = K_m\dot{c}_N/(K_m + c_N)^2$ and $\dot{m}_2 = \tau_2\dot{m}_1/(\tau_1 + \tau_2 m_1)^2$, then $\dot{m}_1$, $\dot{m}_2$ are zero when c_N is maximal. On $[t_{k+j/2}, t_{k+(j+1)/2}]$, $j = 0, 1$, m_i, $i = 1, 2$ can be approximated by*

$$\tilde{m}_i(t) = a_{ij,k}\,(t - t_{k+j/2}) + b_{ij,k},\ \ k = 0,\dots,n,$$

where $t_{k+1/2} = \underset{t\in[t_k,t_{k+1}]}{\operatorname{argmax}}\ c_N(t)$. Computing, we have $t_{1/2} = \tau_c$, and for $k = 1,\dots,n$:

$$t_{k+1/2} = \underset{t\in[t_k,t_{k+1}]}{\operatorname{argmax}}\ c_N(t) = \tau_c + \frac{\sum_{i=1}^{k} R_i\eta_i\, t_i\, e^{t_i/\tau_c}}{\sum_{i=0}^{k} R_i\eta_i\, e^{t_i/\tau_c}}.$$

Imposing $\tilde{m}_i(t_{k+j/2}) = m_i(t_{k+j/2})$ and $\tilde{m}_i(t_{k+(j+1)/2}) = m_i(t_{k+(j+1)/2})$, we get:

$$a_{ij,k} = \frac{m_i(t_{k+(j+1)/2}) - m_i(t_{k+j/2})}{t_{k+(j+1)/2} - t_{k+j/2}},\ \ b_{ij,k} = m_i(t_{k+j/2}).$$

Take $k_s \in \{0,\dots,n\}$, $j_s \in \{0,\dots,p-1\}$ and $t \in [t_{k_s+j_s/p}, t_{k_s+(j_s+1)/p}]$ and let $\Psi(u;i,j)$ be the primitive of $\tilde{m}_2$ on $[t_{i+j/p}, t_{i+(j+1)/p}]$, zero at $t = t_{i+j/p}$. We have for $t \in [t_{k_t+j_t/p}, t_{k_t+(j_t+1)/p}]$:

$$\tilde{M}(t) = \exp\left(-\sum_{k=0}^{k_s-1}\sum_{j=0}^{p-1}[\Psi(u;k,j)]_{t_{k+j/p}}^{t_{k+(j+1)/p}} - \sum_{j=0}^{j_s-1}[\Psi(u;k_s,j)]_{t_{k_s+j/p}}^{t_{k_s+(j+1)/p}} - [\Psi(u;k_s,j_s)]_{t_{k_s+j_s/p}}^{t}\right), \tag{15}$$

and for $s \in [t_{k_s+j_s/p}, t_{k_s+(j_s+1)/p}]$, $t \in [t_{k_t+j_t/p}, t_{k_t+(j_t+1)/p}]$, we get:

$$\begin{aligned}\tilde{M}(t)\tilde{M}^{-1}(s) = \exp\Bigg(&-[\Psi(u;k_s,j_s)]_s^{t_{k_s+j_s/p}} + \sum_{j=0}^{j_s-1}[\Psi(u;k_s,j)]_{t_{k_s+j/p}}^{t_{k_s+(j+1)/p}} - \sum_{j=0}^{j_t-1}[\Psi(u;k_t,j)]_{t_{k_t+j/p}}^{t_{k_t+(j+1)/p}}\\ &- \sum_{i=k_s}^{k_t-1}\sum_{j=0}^{p-1}[\Psi(u;i,j)]_{t_{i+j/p}}^{t_{i+(j+1)/p}} - [\Psi(u;k_t,j_t)]_{t_{k_t+j_t/p}}^{t}\Bigg).\end{aligned} \tag{16}$$

To integrate the product $\tilde{M}(t)\tilde{M}^{-1}(s)\tilde{m}_1(s)$ with respect to s, we gather the terms depending on s in (16) together and we get, for $t \in [t_{k_t+j_t/p}, t_{k_t+(j_t+1)/p}]$:

$$\begin{aligned}&\int_{t_{k_s+j_s/p}}^{t_{k_s+(j_s+1)/p}} \tilde{M}(t)\tilde{M}^{-1}(s)\,\tilde{m}_1(s)\,\mathrm{d}s = \int_{t_{k_s+j_s/p}}^{t_{k_s+(j_s+1)/p}} \exp\left(\Psi(s;k_s,j_s)\right)\ \tilde{m}_1(s)\,\mathrm{d}s\\ &\exp\left(-\Psi(t;k_t,j_t) + \sum_{j=0}^{j_s-1}\Psi(t_{k_s+(j+1)/p};k_s,j) - \sum_{j=0}^{j_t-1}\Psi(t_{k_t+(j+1)/p};k_t,j) - \sum_{i=k_s}^{k_t-1}\sum_{j=0}^{p-1}\Psi(t_{i+(j+1)/p};i,j)\right).\end{aligned} \tag{17}$$

Consequently, we obtain an approximation of F on $[t_{k_t+j_t/p}, t_{k_t+(j_t+1)/p}]$, $k_t = 0, \dots, n$, $j_t = 0, \dots, p-1$ writing:

$$\begin{aligned}\tilde{F}(t)/A0 &= \int_0^t \tilde{M}(t)\tilde{M}^{-1}(s)\,\tilde{m}_1(s)\,\mathrm{d}s \\ &= \sum_{i=0}^{k_t-1}\sum_{j=0}^{p-1}\int_{t_{i+j/p}}^{t_{i+(j+1)/p}} \tilde{M}(t)\tilde{M}^{-1}(s)\,\tilde{m}_1(s)\,\mathrm{d}s + \sum_{j=0}^{j_t-1}\int_{t_{k_t+j/p}}^{t_{k_t+(j+1)/p}} \tilde{M}(t)\tilde{M}^{-1}(s)\,\tilde{m}_1(s)\,\mathrm{d}s \\ &+ \int_{t_{k_t+j_t/p}}^{t} \tilde{M}(t)\tilde{M}^{-1}(s)\,\tilde{m}_1(s)\,\mathrm{d}s.\end{aligned} \tag{18}$$

Proposition 18 *Choosing $\tilde{m}_1$ as a piecewise polynomial function and $\tilde{m}_2$ as a piecewise constant function on $[0,T]$, the function:*

$$\tilde{F}(t) = A\int_0^t \tilde{M}(t)\tilde{M}^{-1}(s)\,\tilde{m}_1(s)\,\mathrm{d}s,$$

where $\tilde{M}(t) = \exp\left(-\int_0^t \tilde{m}_2(s)\,\mathrm{d}s\right)$, has a closed-form expression in the polynomial-exponential category.

PROOF. Decomposing the integral (18) as a sum of integrals over the partition $(t_{i+j/p})_{ij}$ gives the expression:

$$\begin{aligned}\tilde{F}(t)/A &= \sum_{i=0}^{k_t-1}\sum_{j=0}^{p-1}\int_{t_{i+j/p}}^{t_{i+(j+1)/p}} \tilde{M}(t)\tilde{M}^{-1}(s)\,\tilde{m}_1(s)\,\mathrm{d}s \\ &+ \sum_{j=0}^{j_t-1}\int_{t_{k_t+j/p}}^{t_{k_t+(j+1)/p}} \tilde{M}(t)\tilde{M}^{-1}(s)\,\tilde{m}_1(s)\,\mathrm{d}s \\ &+ \int_{t_{k_t+j_t/p}}^{t} \tilde{M}(t)\tilde{M}^{-1}(s)\,\tilde{m}_1(s)\,\mathrm{d}s,\end{aligned} \tag{19}$$

for $t \in [t_{k_t+j_t/p}, t_{k_t+(j_t+1)/p}]$, $k_t = 0, \dots, n$, $j_t = 0, \dots, p-1$, and each of this integral term belongs to the polynomial-exponential category.

Remark 19 *To construct $\tilde{F}$, the functions m_1 and m_2 were considered independently in the sense that the approximation does not rely on the relation (6) between m_1 and m_2. A direct consequence is that an upper approximation of the force can be obtained from an upper approximation of m_1. Outside the scope of this paper, this method may be applied for more general non-autonomous models.*

Proposition 20 *Adding a real parameter ν to the functions $\tilde{m}_1, \tilde{m}_2$ as follows*

$$\breve{\tilde{m}}_1(t;\nu) = \frac{c_N(t)}{\nu\,K_m + c_N(t)} \text{ and } \breve{\tilde{m}}_2(t;\nu) = \frac{\nu}{\tau_1 + \tau_2\,m_1(t)}$$

allows to construct an upper (or lower) approximation $\tilde{F}$ of F parameterized by ν.

Remark 21 *A naive approach is to use classic integration schemes to define an explicit expression for $\tilde{F}$. Namely, using an explicit Euler scheme for the force equation (7) adapted to the partition $(t_{i+j/p})_{ij}$ gives:*

$$\tilde{F}(t_{i+(j+1)/p}) = \tilde{F}(t_{i+j/p})\,c_{i,j} + A\,d_{i,j},$$

where $c_{ij} = (1 - h_{i,j}\,m_2(t_{i+j/p}))$, $h_{i,j} = t_{i+(j+1)/p} - t_{i+j/p}$ and $d_{ij} = m_1(t_{i+j/p})$ for $i = 0, \dots, n$ and $j = 0, \dots, p-1$.

We deduce the following explicit expression for $\tilde{F}(t_{k_t+j_t/p}),\ k_t = 0,\dots,n,\ j_t = 0,\dots p-1$*:*

$$\tilde{F}(t_{k_t+j_t/p})/A = \sum_{j=0}^{j_t-1} h_{k_t,j}\, d_{k_t,j} \prod_{j'=j+1}^{j_t-1} c_{k_t,j'} + \sum_{i=0}^{k_t-1}\sum_{j=0}^{p-1} h_{i,j}\, d_{i,j} \left(\prod_{j'=0}^{p-1} \prod_{i'=i+1}^{k_t-1} c_{i',j'} \prod_{j'=j+1}^{p-1} c_{i,j'} \prod_{j'=0}^{j_t-1} c_{k_t,j'} \right). \tag{20}$$

However, such method is not adapted for the design of our electrostimualtor (see Section 6). Indeed, it does not exploit the structure of the Hill functions m_1 *and* m_2 *and yields worse results – in terms of time complexity and approximation error – compared to the approximation* (18)*.*

Error estimate.

We give a bound on the error between the approximation $\tilde{F}$ and F in the case where $\tilde{m_2}_{|[t_k,t_{k+1}]}$ is the average of m_2 on $[t_k, t_{k+1}]$.

Proposition 22 *Consider the case where* $0 \le \tilde{m}_1(t) \le 1$ *and* $\tilde{m}_2$ *is equal to the average of* m_2 *on* $[t_j, t_{j+1}]$*,* $j = 0,\dots,n$*. Assume moreover that each restriction on* $[t_j, t_{j+1}]$*,* $j = 0,\dots,n$ *of* m_1 *(resp.* m_2*) is concave (resp. convex). Then, the error between the force* F *and its approximation* $\tilde{F}$ *defined by* (18) *satisfies for* $k = 0,\dots,n$*:* $|F(t_k) - \tilde{F}(t_k)|/A \le \int_0^{t_k} |m_1(s) - \tilde{m}_1(s)|\,\mathrm{d}s + t_k \int_0^{t_k} |m_2(s) - \tilde{m}_2(s)|\,\mathrm{d}s.$

Proof 1 *For* $t_k > s$*, we have:*

$$\begin{aligned}
|F(t_k) - \tilde{F}(t_k)|/A_0 &= \left| \int_0^{t_k} M(t_k)M^{-1}(s)m_1(s) - \tilde{M}(t_k)\tilde{M}^{-1}(s)\tilde{m}_1(s)\,\mathrm{d}s \right| \\
&\le \int_0^{t_k} M(t_k)M^{-1}(s)|m_1(s) - \tilde{m}_1(s)|\,\mathrm{d}s + \left| \int_0^{t_k} \tilde{m}_1(s)M(t_k)M^{-1}(s) - \tilde{M}(t_k)\tilde{M}^{-1}(s)|\,\mathrm{d}s \right| \\
&\le \int_0^{t_k} |m_1(s) - \tilde{m}_1(s)|\,\mathrm{d}s + \left| \int_0^{t_k} M(t_k)M^{-1}(s) - \tilde{M}(t_k)\tilde{M}^{-1}(s)\,\mathrm{d}s \right|. \\
&= \int_0^{t_k} |m_1(s) - \tilde{m}_1(s)|\,\mathrm{d}s + \left| \int_0^{t_k} \exp\left(-\int_s^{t_k} m_2(u)\,\mathrm{d}u\right) - \exp\left(-\int_s^{t_k} \tilde{m}_2(u)\,\mathrm{d}u\right)\,\mathrm{d}s \right| \\
&= \int_0^{t_k} |m_1(s) - \tilde{m}_1(s)|\,\mathrm{d}s + \left| \sum_{i=0}^{k-1} \int_{t_i}^{t_{i+1}} \exp\left(-\int_s^{t_k} m_2(u)\,\mathrm{d}u\right) - \exp\left(-\int_s^{t_k} \tilde{m}_2(u)\,\mathrm{d}u\right)\,\mathrm{d}s \right|.
\end{aligned}$$

Recall the function m_2 *is decreasing on* $[t_i, s_i]$ *and increasing on* $[s_i, t_{i+1}]$ *where* s_i *is the unique maximum of* c_N *on* $[t_i, t_{i+1}]$*. Define* $\xi(s) \coloneqq \tilde{m}_2(s) - m_2(s)$*. Since* m_2 *is convex on* $[t_i, t_{i+1}]$*, we have three cases:*

(i) $\int_{t_i}^{s} \xi(u)\,\mathrm{d}u \le 0$ *for* $s \in [t_i, t_{i+1}]$. *We have, for* $i = 0, \ldots, k-1$,

$$\begin{aligned}
&\left| \int_{t_i}^{t_{i+1}} \exp\left(-\int_s^{t_k} m_2(u)\,\mathrm{d}u\right) - \exp\left(-\int_s^{t_k} \tilde{m}_2(u)\,\mathrm{d}u\right)\,\mathrm{d}s \right| \\
&\qquad = \left| \int_{t_i}^{t_{i+1}} \exp\left(\int_{t_k}^{s} m_2(u)\,\mathrm{d}u\right)\left(1 - \exp\left(\int_{t_k}^{s} \xi(u)\,\mathrm{d}u\right)\right)\,\mathrm{d}s \right| \\
&\qquad \le \int_{t_i}^{t_{i+1}} \left| 1 - \exp\left(\int_{t_i}^{s} \xi(u)\,\mathrm{d}u\right) \right| \mathrm{d}s, \ \textit{(since } \int_{t_j}^{t_{j+1}} \xi(u)\,\mathrm{d}u = 0\textit{)} \\
&\qquad \le \int_{t_i}^{t_{i+1}} \int_{t_i}^{s} -\xi(u)\,\mathrm{d}u\,\mathrm{d}s \\
&\qquad \le (t_{i+1} - t_i) \int_{t_i}^{t_{i+1}} |\xi(u)|\,\mathrm{d}u.
\end{aligned} \tag{21}$$

(ii) $\int_{t_i}^{s} \xi(u)\,\mathrm{d}u \ge 0$ *for* $s \in [t_i, t_{i+1}]$. *We obtain the same inequality as in the case (i) by replacing* ξ *by* $-\xi$.

(iii) There exists an unique $\theta_i \in [t_i, t_{i+1}]$ *such that* $\int_{t_i}^{s} \xi(u)\,\mathrm{d}u \le 0$ *for* $s \in [t_i, \theta_i]$ *and* ≥ 0 *for* $s \in [\theta_i, t_{i+1}]$. *Write*

$$\begin{aligned}
&\left| \int_{t_i}^{t_{i+1}} \exp\left(-\int_s^{t_k} m_2(u)\,\mathrm{d}u\right) - \exp\left(-\int_s^{t_k} \tilde{m}_2(u)\,\mathrm{d}u\right)\,\mathrm{d}s \right| \\
&\qquad \le \left| \int_{t_i}^{\theta_i} \exp\left(-\int_s^{t_k} m_2(u)\,\mathrm{d}u\right) - \exp\left(-\int_s^{t_k} \tilde{m}_2(u)\,\mathrm{d}u\right)\,\mathrm{d}s \right| \\
&\qquad\qquad + \left| \int_{\theta_i}^{t_{i+1}} \exp\left(-\int_s^{t_k} m_2(u)\,\mathrm{d}u\right) - \exp\left(-\int_s^{t_k} \tilde{m}_2(u)\,\mathrm{d}u\right)\,\mathrm{d}s \right|
\end{aligned} \tag{22}$$

We have: $\int_{\theta_i}^{s} \xi(u)\,\mathrm{d}u \le 0$ *for* $s \in [t_i, \theta_i]$ *and* ≥ 0 *for* $s \in [\theta_i, t_{i+1}]$. *As in the case (i), the first integral in the right hand side of* (22) *is bounded by* $(\theta_i - t_i) \int_{t_i}^{\theta_i} |\xi(u)|\,\mathrm{d}u$. *Likewise, the second integral in the right hand side of* (22) *is bounded by* $(t_{i+1} - \theta_i) \int_{\theta_i}^{t_{i+1}} |\xi(u)|\,\mathrm{d}u$.

This concludes the proof.

5 Numerical solution to optimization problems

5.1 Functional specification for the computation of a pulses train

The aim is to compute a local minimum $\sigma^* = (\eta_0^*, \ldots, \eta_n^*, t_1^*, \ldots, t_n^*, T) \in \mathbb{R}_+^{2n+2}$ of a cost function denoted as Θ. The free final time T adjusts automatically the optimal frequency of the pulses train. The functional specification of the electrostimulator imposes efficient computation of this minimum (real time computation) and this prevents us (at least when Θ involves the force) from using direct or indirect methods such as those presented in [2], mainly because these methods are based on a numerical scheme to approximate the variable F.

5.2 Finite dimensional optimization methods

We recall basic facts about finite dimensional optimization, see [5] for details, to emphasize that an optimal sampled-data control problem can be viewed as an instance of such optimization problem.

The optimization problems, associated to the optimal sampled-data control problems **OCP1** and **OCP2** presented in Section 3.2, can be written in the form:

$$\begin{aligned} \min_{\sigma} \ & \Theta(\sigma) \\ & \Im(\sigma) \leq 0, \end{aligned} \tag{23}$$

where $\Im(\sigma) = (\Xi_1(\sigma), \dots, \Xi_{3n+5}(\sigma))$ is the vector of constraints defined by:

$$\begin{aligned} &\Xi_i(\sigma^*) = t^*_{i-1} - t^*_i + I_{\min},\ i = 1, \dots n, \\ &\Xi_{n+1}(\sigma^*) = t^*_n - T, \\ &\Xi_{n+2+i}(\sigma^*) = -\eta^*_i,\ i = 0, \dots n+1, \\ &\Xi_{2n+4+i}(\sigma^*) = \eta^*_i - 1,\ i = 0, \dots n+1. \end{aligned}$$

The cost $\Theta : \sigma \mapsto \Theta(\sigma)$ related to the endurance or the force strengthening program is smooth with respect to σ. Consider the Lagrangian defined for all $(\sigma, \mu) \in \mathbb{R}^{2n+1} \times \mathbb{R}_+^{3n+5}$ by:

$$\mathcal{L}(\sigma, \mu) \coloneqq \Theta(\sigma) + \mu \cdot \Im(\sigma).$$

The problem (23) is equivalent to the primal problem

$$\inf_{\sigma \in \mathbb{R}^{2n+1}} \sup_{\mu \in {\mathbb{R}_+}^{3n+5}} \mathcal{L}(\sigma, \mu)$$

and the first order necessary optimality conditions for σ^* to be a local minimizer, assuming the vectors $\Xi_i'(\sigma^*),\ i \in \{i,\ \Xi_i(\sigma^*) = 0\}$ to be linearly independent, state that there exists a Lagrange multiplier $\lambda \in \mathbb{R}^{3n+5}$ such that

$$\begin{aligned} &\nabla_\sigma \Theta(\sigma^*) + \lambda \cdot \Im(\sigma^*) = 0,\ \lambda \cdot \Im(\sigma^*) = 0 \\ &\lambda_i \geq 0,\ \Xi_i(\sigma^*) \leq 0,\ i = 1, \dots, 3n+5. \end{aligned}$$

We usually do not solve directly these optimality conditions to compute an optimal pair (σ^*, λ^*), but a relaxation of these conditions can lead to efficient algorithm, namely the primal-dual interior point method [5].

5.3 Force optimization

We consider the problems the endurance and force strengthening optimization problems **OCP1** and **OCP2**. For each problem, we give the approximation $\tilde{\Theta}$ of the cost functions Θ based on the approximation $\tilde{F}$ of the variable F described in section 4. We solve the associated problem (23) – where Θ is replaced by $\tilde{\Theta}$ – using an interior point method on a standard computer [1]. Note that $\tilde{\Theta}$ may consist of million of bytes, for that reason it is crucial to use an approximation of the gradient of $\tilde{\Theta}$ with respect to $t_i,\ i = 1, \dots, n$, computed via finite differences (vs formal computation). We initialize the pulses train to a regular partition of $[0, 1]$ and the initial amplitudes being equal to 1.

We consider the force approximation $\tilde{F}$ defined by (18) taking the piecewise affine functions $\tilde{m}_1, \tilde{m}_2$ to be equal on $[t_k, t_{k+1}]$, $k = 0, \dots, n$ to:

$$\tilde{m}_1(t) = \begin{cases} m_1(t_{k+1/2}) & \text{if } t \in [t_k, t_{k+1/2}] \\ a_{1j,k}\,(t - t_{k+1}) + b_{1j,k}, & \text{if } t \in [t_{k+1/2}, t_{k+1}] \end{cases},$$

$$\tilde{m}_2(t) = \begin{cases} \frac{m_2(t_k) + m_2(t_{k+1/2})}{2} & \text{if } t \in [t_k, t_{k+1/2}] \\ \frac{m_2(t_{k+1/2}) + m_2(t_{k+1})}{2}, & \text{if } t \in [t_{k+1/2}, t_{k+1}] \end{cases},$$

where $t_{k+1/2} = \underset{u \in [t_k, t_{k+1}]}{\operatorname{argmax}}\ c_N(u)$, $a_{1j,k} = (m_1(t_{k+1}) - m_1(t_{k+1/2}))/(t_{k+1} - t_{k+1/2})$ and $b_{1j,k} = m_1(t_{k+1})$.

[1] 4 Intel@Core^{TM} i5 CPU @ 2.4Ghz

5.3.1 Problem OCP1: $\Theta(\sigma) \coloneqq -F(T)$.

Approximated cost. The objective function $\Theta(\sigma) = -F(T)$ is approximated by the function $\tilde{\Theta}(\sigma) = -\tilde{F}(T)$. The optimization variables consist in the impulse times while the amplitudes are fixed to 1.

Numerical result: The optimal solution σ^*, the force response F and its approximation $\tilde{F}$ are depicted in Fig.1.

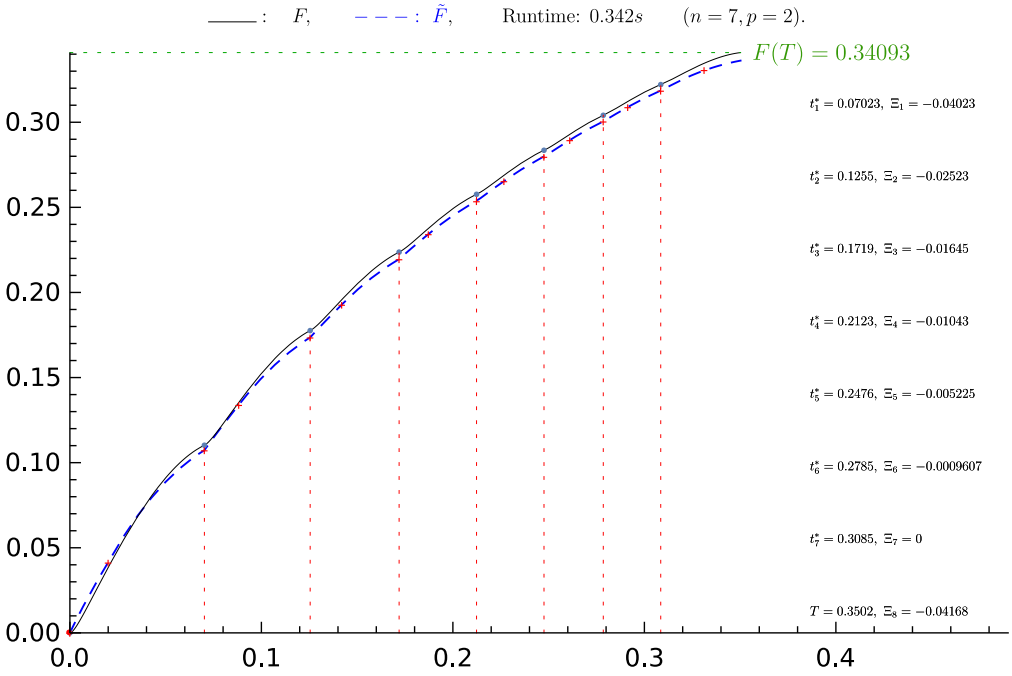

Fig. 1. The dashed curve is the time evolution of F associated to the optimal solution $\sigma^* = (t_1^*, \ldots, t_n^*, T)$ of $\max_\sigma \tilde{F}(T)$ (T free) (see (18) for the definition of $\tilde{F}$) under the constraints $\Xi_i \leq 0,\ i = 1, \ldots, n+1$ (see (23)). The continuous curve is the response $t \mapsto F(t)$ to σ^*. Values of the constants are $\tau_c = 20\text{ms}$, $n = 7$, $I_{\min} = 20\text{ms}$.

5.3.2 Problem OCP2: $\Theta(\sigma) \coloneqq \displaystyle\int_0^T |F(t) - F_{ref}|^2 \, \mathrm{d}t$.

The cost $\Theta(\sigma) = \displaystyle\int_0^T |F(s) - F_{ref}|^2 \, \mathrm{d}s$ is approximated by:

$$\tilde{\Theta}(\sigma) = \sum_{k=0}^{n} \left(\tilde{F}(t_{k+1}) - F_{ref}\right)^2 (t_{k+1} - t_k),$$

where the functions $\tilde{m}_1$ and $\tilde{m}_2$ are replaced by $\breve{\tilde{m}}_1(t; 0.95)$ and $\breve{\tilde{m}}_2(t; 0.95)$ respectively (see Proposition 20 for their definition).

Numerical result: The optimal solution σ^*, the force response F and its approximation $\tilde{F}$ are depicted in Fig.2.

5.4 Ca^{2+} concentration optimization

Uniqueness of the optimal solution:

Fix $\eta_i = 1, i = 0, \ldots, n$. The cost function $\Theta(\sigma) = \displaystyle\int_0^T (c_N(s) - c_{ref})^2 \, \mathrm{d}s$ is smooth with respect to t_1 and not convex on $[0, T]$.

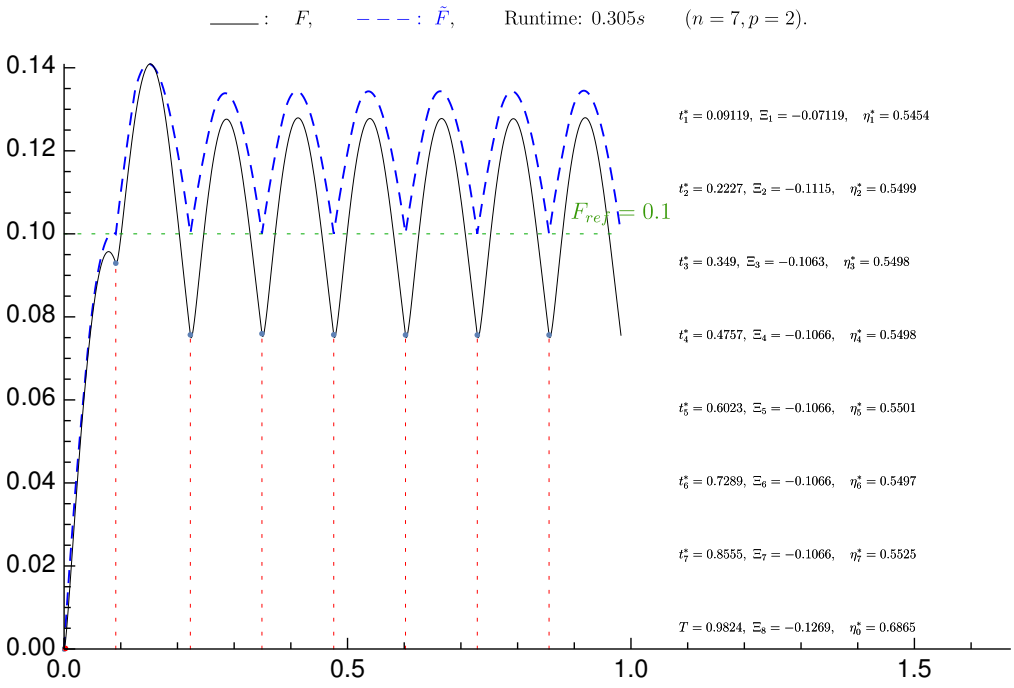

Fig. 2. The dashed curve is associated to the optimal solution $\sigma^* = (\eta_0^*, \ldots, \eta_n^*, t_1^*, \ldots, t_n^*, T)$ of $\min_\sigma \sum_{k=0}^n \left(\tilde{F}(t_{k+1}) - F_{ref}\right)^2 (t_{k+1} - t_k)$ ($T = t_{n+1}$ is free), where $\tilde{F}$ is the upper approximation of F as described from Proposition 20 under the constraints $\Xi_i \leq 0,\ i = 1, \ldots, 3n+5$ (see (23)). The continuous curve is the response $t \mapsto F(t)$ to σ^*. Values of the constants are $\tau_c = 20$ms, $n = 5$, $I_{\min} = 20$ms, $\nu = 0.95$ and $F_{ref} = 0.1$kN.

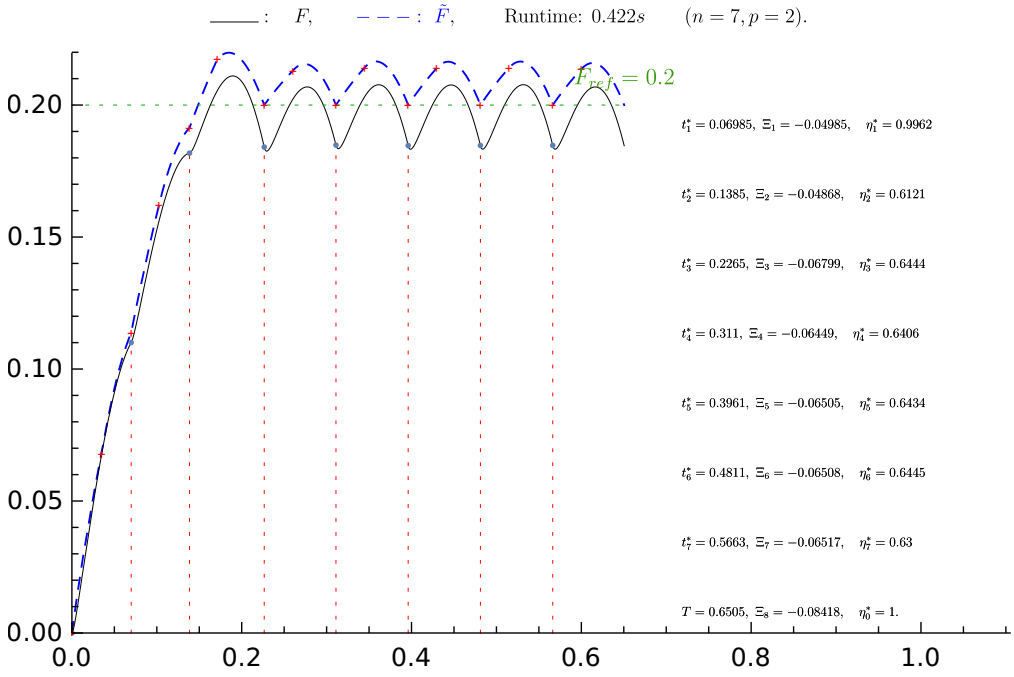

Fig. 3. The dashed curve is associated to the optimal solution $\sigma^* = (\eta_0^*, \ldots, \eta_n^*, t_1^*, \ldots, t_n^*)$ of $\min_\sigma \sum_{k=0}^n \left(\tilde{F}(t_{k+1}) - F_{ref}\right)^2 (t_{k+1} - t_k)$ ($T = t_{n+1}$ is free), where $\tilde{F}$ is the approximated force given by (18), under the constraints $\Xi_i \leq 0,\ i = 1, \ldots, 3n+5$ (see (23)). The continuous curve is the response $t \mapsto F(t)$ to σ^*. Values of the constants are $\tau_c = 20$ms, $n = 7$, $I_m = 20$ms and $F_{ref} = 0.2$kN.

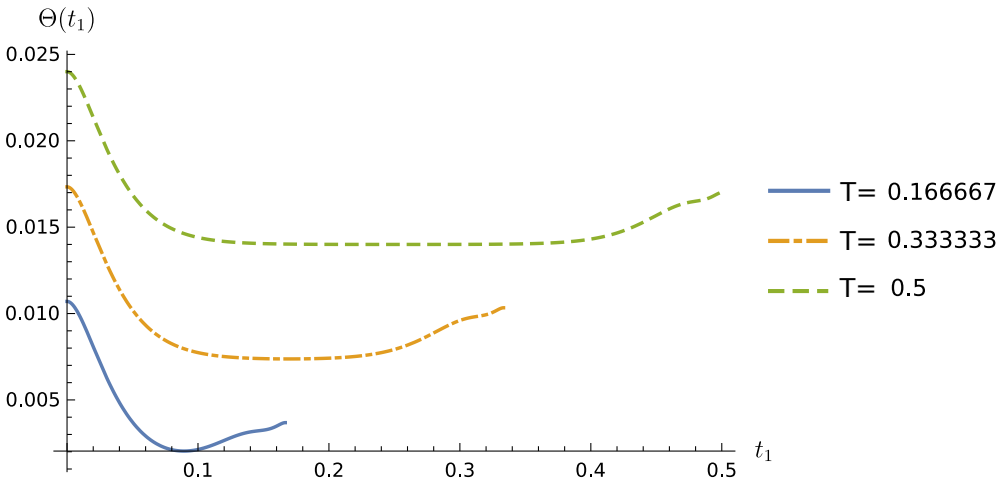

Fig. 4. Objective function $\Theta(\sigma) = \int_0^T (c_N(s) - c_{ref})^2 \, \mathrm{d}s$, where T is assigned to specific values. Constants for these simulations are $\tau_c = 20\text{ms}$, $n = 1$, $I_m = 20\text{ms}$.

In Fig.4, we plot for $n = 1$ the objective function $\Theta(t_1)$ and for T fixed at some specific values.

The well-posedness of this optimization problem for any number n of impulsions times can be shown by inductive reasoning.

5.4.1 Cost: $\Theta(\sigma) = -c_N(T)$.

True cost. We have an explicit expression for c_N, this problem can be easily solved numerically. We consider the finite dimensional optimization problem 23 where the cost is

$$\Theta(\sigma) = \sum_{i=0}^{n} R_i (T - t_i) \, e^{-\frac{T-t_i}{\tau_c}}.$$

(Note that the amplitudes are fixed to 1).

Numerical result: Fig. 5 represents the time evolution of c_N associated to (locally) optimal impulse times.

5.4.2 Cost: $\Theta(\sigma) = \int_0^T |c_N(t) - c_{ref}|^2 \, \mathrm{d}t$, *$T$ free.*

In this case, we approximate Θ by

$$\tilde{\Theta}(\sigma) = \sum_{i=0}^{n} (\bar{c}_N^i - c_{N,ref})^2 (t_{i+1} - t_i), \tag{24}$$

where the amplitudes and T are free and $\bar{c}_N$ is given by Proposition 9.

Numerical result: The optimal solution σ^* and its response c_N are depicted in Fig. 6.

6 Isometric case: design of a smart muscular electrostimulator

In this section we apply our study in the isometric case associated to the conception of a smart electrostimulator. In this case, the task is to assign a constant reference force, but the general frame is suboptimal motion planning, see [11,12] for the theoretical foundations.

Advanced commercial muscular electrostimulator for training or reeducation purposes are based on the following. First of all, the user defines a program training. Basically endurance program with low frequency sequences of trains

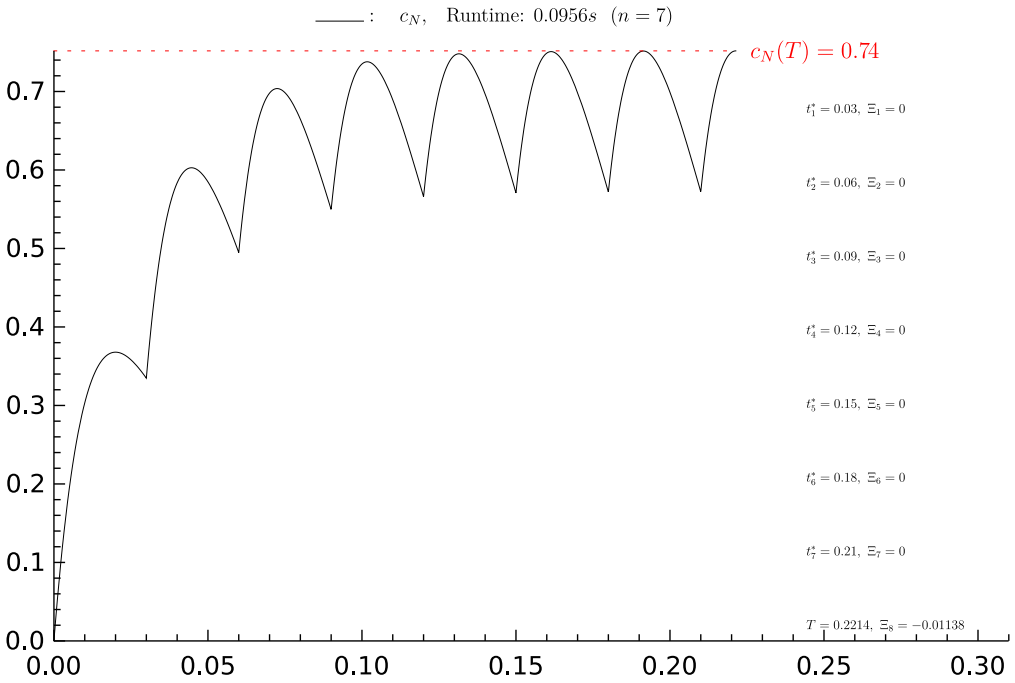

Fig. 5. Time evolution of c_N associated to the optimal sampling times σ^* for $\max_\sigma c_N(T)$ (T free) under the constraints $\Xi_i \leq 0,\ i = 1, \ldots, n+1$ (see (23)). Values of the constants are $\tau_c = 20$ms, $n = 7$, $I_m = 20$ms.

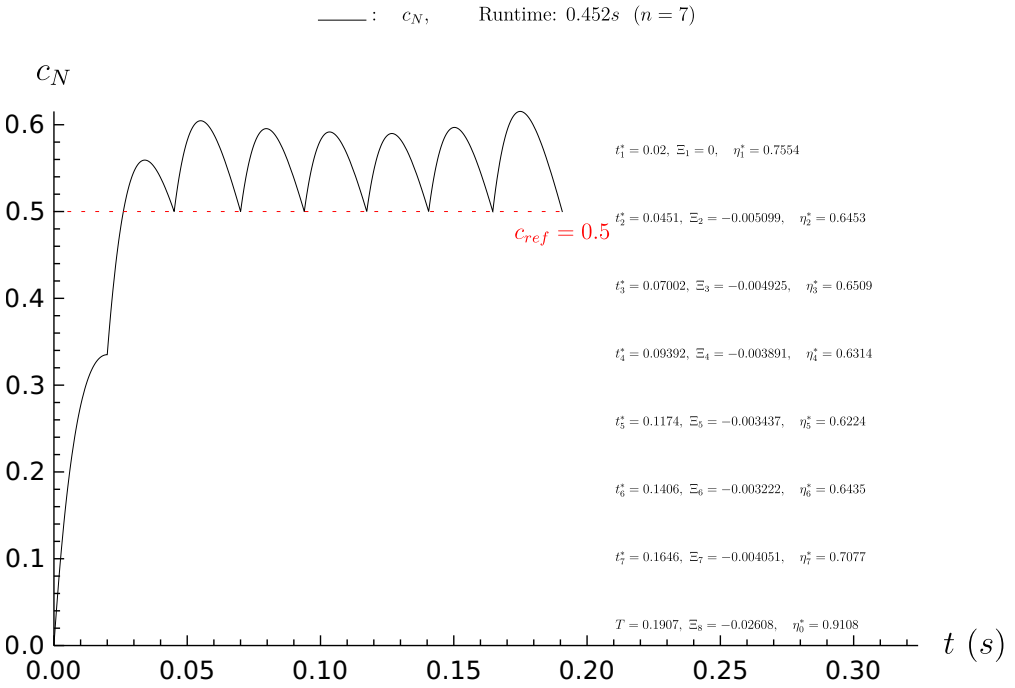

Fig. 6. The dashed curve is the time evolution of c_N associated to the optimal solution $\sigma^* = (\eta_0^*, \ldots, \eta_n^*, t_1^*, \ldots, t_n^*)$ of $\min_\sigma \sum_{i=0}^n (\bar{c}_N^i - c_{N,ref})^2 (t_{i+1} - t_i)$ (T free), where $\bar{c}_N$ is defined in Proposition 9, under the constraints $\Xi_i \leq 0,\ i = 1, \ldots, 3n+5$ (see (23)). The continuous curve is the response $t \mapsto c_N(t)$ to σ^*. Constants for these simulations are $\tau_c = 20$ms, $n = 7$, $I_m = 20$ms and $c_{ref} = 0.5$.

Table 1
List of variables and values of the constant parameters in the Ding et al. model

Symbol	Unit	Value	Description
C_N	—	—	Normalized amount of Ca^{2+}-troponin complex
F	kN	—	Force generated by muscle
t_i	s	—	Time of the i^{th} pulse
n	—	—	Total number of the pulses before time t
i	—	—	Stimulation pulse index
τ_c	s	0.02	Time constant that commands the rise and the decay of C_N
$\bar{R}$	—	1.143	Term of the enhancement in C_N from successive stimuli
A	$\mathrm{kN}\cdot s^{-1}$	—	Scaling factor for the force and the shortening velocity of muscle
τ_1	s	50.95	Force decline time constant when strongly bound cross-bridges absent
τ_2	s	0.1244	Force decline time constant due to friction between actin and myosin
K_m	—	—	Sensitivity of strongly bound cross-bridges to C_N
A_{rest}	$\mathrm{kN}\cdot s^{-1}$	3.009	Value of the parameter A when muscle is not fatigued
α_A	s^{-2}	$-4.0\ 10^{-1}$	Coefficient for the force-model parameter A in the fatigue model
τ_{fat}	s	127	Time constant controlling the recovery of A

(with constant interpulse) or force strengthening with high frequency trains. The program is a sequence of trains or rest periods. Before starting, the muscle is scanned to determine the parameters. A smart electrostimulator based on our study aims to design automatically such sequence, each program being translated into an optimization problem. Besides, in our framework, one can used VFT (Variable Frequency Trains) vs CFT (Constant Frequency Trains) in the standard case to complete the tuning of the amplitude.

One needs the following proposition associated to the endurance program presented in Fig.7 to illustrate the smart electrostimulator conception.

Proposition 23 *Consider the endurance program, where a reference force F_{ref} is given. Plugging such F_{ref} in $\dot{F}=0$ leads to solve the equation: $A\tau_2 m_1^2 + A\tau_1 m_1 - F_{ref} = 0$, which has an unique positive root m_1^+ giving the reference concentration $c_{N,ref}$. This root is stable and leads to design an optimized pulses train solving the L^2-optimization problem with cost: $\int_0^T |c_N(t) - c_{N,ref}|^2 \,\mathrm{d}t$.*

PROOF. Note that the mapping m_1: $c_N \mapsto m_1(c_N)$ is one-to-one and m_1 can be taken as an accessory control in place of c_N. Solving in m_1 the equation $\dot{F}=0$ leads to real roots denoted respectively $m_1^+ > 0$ and $m_1^- < 0$. Taking m_1^+, stability is granted since $\lambda = -m_2(c_N^+)$ is negative, where c_N^+ is given by $m_1(c_N^+) = m_1^+$. □

Remark 24 *The optimization problem $\min_\sigma \int_0^T |c_N(t) - c_{N,ref}|^2 \,\mathrm{d}t$ can be efficiently solved using the piecewise constant approximation of c_N of Proposition 9. Indeed, we have:*

$$\int_0^T |c_N(t) - c_{N,ref}|^2 \,\mathrm{d}t \approx \sum_{i=0}^{n} (\bar{c}_N^i - c_{N,ref})^2 (t_{i+1} - t_i).$$

7 Conclusion

In this short article, we have mainly presented a finite dimensional approximation of the muscular force response to FES-input exploiting the mathematical structure of the model. The construction is based on the Ding et al. model but can be adapted to deal with the different models discussed in [19]. We have presented one application of our study related to motion planning in the isometric case in view to design a smart electrostimulator, which is an ongoing industrial project. Our approximation can be used to parameters estimation [19,17] and to design MPC-optimized sampled-data control schemes, applying standard algorithms [16,18] to this situation.
Another application of our study is to track in the non-isometric case a path in the joint angle variable and this will be developed in a forthcoming article.

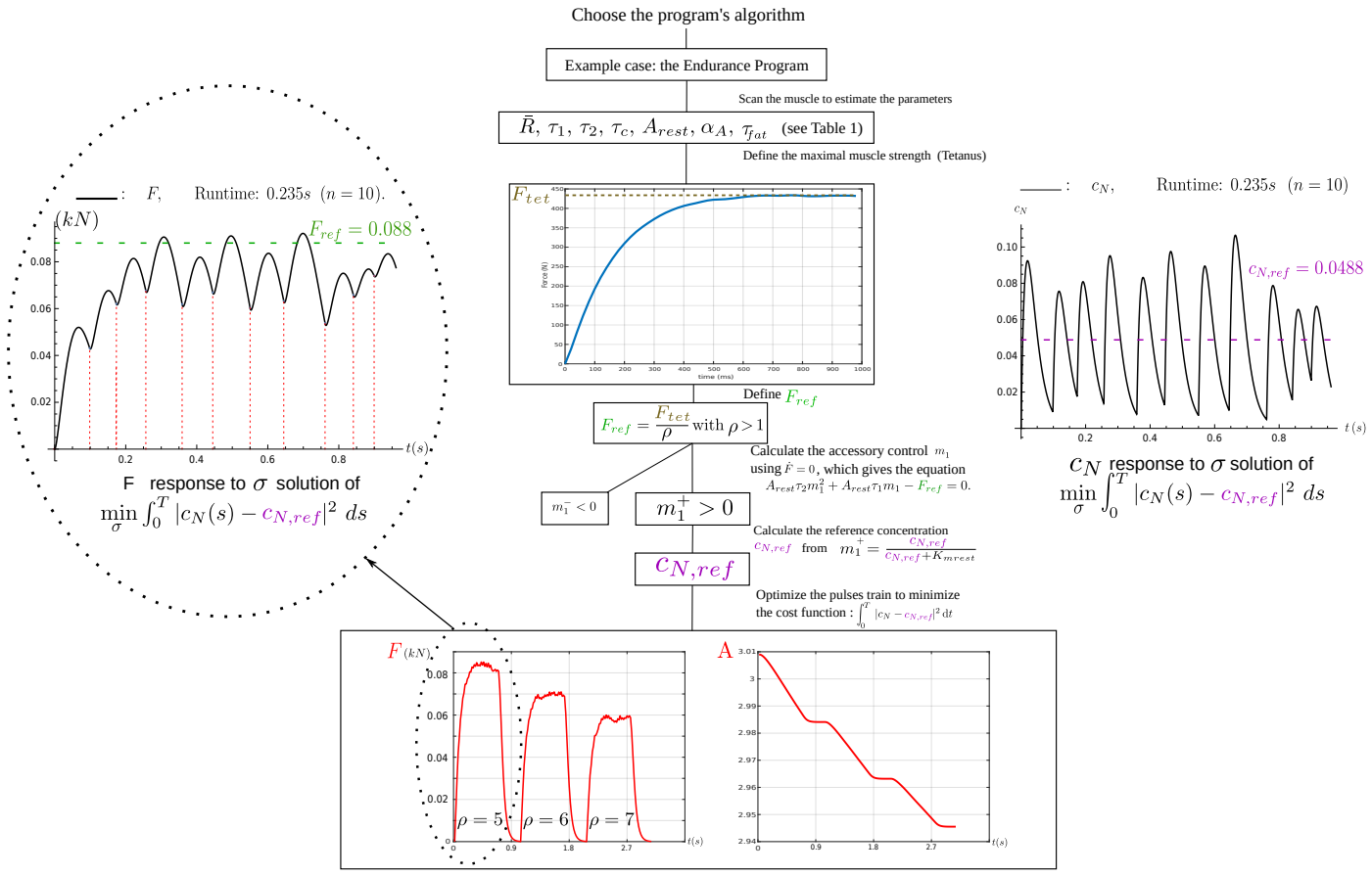

Fig. 7. Endurance program for a smart electrostimulator.

References

[1] Bakir T., Bonnard B. & Rouot J. (2019). A case study of optimal input-output system with sampled-data control: Ding et al. force and fatigue muscular control model. *Netw. Hetero. Media*, **14**(1), 79–100.

[2] Bakir T., Bonnard B., Bourdin L. & Rouot J. (2020). Pontryagin-type conditions for optimal muscular force response to functional electrical stimulations. *J. Optim. Theory Appl.*, **184**, 581–602.

[3] Bonnard B. & Rouot J. (2020). Geometric optimal techniques to control the muscular force response to functional electrical stimulation using a non-isometric force-fatigue model. *Journal of Geometric Mechanics, American Institute of Mathematical Sciences (AIMS)*.

[4] Bourdin L. & Trélat E. (2016). Optimal sampled-data control, and generalizations on time scales. *Math. Cont. Related Fields*, **6**, 53–94.

[5] Boyd S. & Vandenberghe L. (2004). Convex Optimization. *Cambridge, U.K.: Cambridge Univ. Press.*

[6] Doll B.D. , Kirsch N.A. & Sharma N. (2015). Optimization of a Stimulation Train based on a Predictive Model of Muscle Force and Fatigue. *IFAC-PapersOnLine*, **48**(20), 338–342.

[7] Ding J., Wexler A.S. & Binder-Macleod S.A. (2000). Development of a mathematical model that predicts optimal muscle activation patterns by using brief trains. *J. Appl. Physiol.*, **88**, 917–925.

[8] Ding J., Wexler A.S. & Binder-Macleod S.A. (2002). A predictive fatigue model. I. Predicting the effect of stimulation frequency and pattern on fatigue. IEEE Transactions on Neural Systems and Rehabilitation Engineering, **10**(1), 48–58.

[9] J. Ding, A.S. Wexler & S.A. Binder-Macleod, A predictive fatigue model. II. Predicting the effect of resting times on fatigue. IEEE Transactions on Neural Systems and Rehabilitation Engineering, **10** no.1 (2002), 59–67.

[10] R. Gesztelyi, J. Zsuga, A. Kemeny-Beke, B. Varga, B. Juhasz & A. Tosaki, The Hill equation and the origin of quantitative pharmacology. *Archive for history of exact sciences*, **66** no. 4 (2012), 427–438.

[11] Hirschorn, R. M. & Davis, J. H., Output tracking for nonlinear systems with singular points. SIAM J. Control Optim. 25 (1987), no. 3, 547–557.

[12] Hirschorn, R. M. & Davis, J. H., Global output tracking for nonlinear systems. SIAM J. Control Optim. 26 (1988), no. 6, 1321–1330.

[13] Isidori A. (1995). Nonlinear Control Systems. *3rd ed. Berlin, Germany: Springer-Verlag.*

[14] Marion M.S., Wexler A.S. & Hull M.L. (2013). Predicting non-isometric fatigue induced by electrical stimulation pulse trains as a function of pulse duration. *Journal of neuroengineering and rehabilitation*, **10**(1).

[15] Michaelis L. & Menten M.L. (1913). Die Kinetik der Intertinwerkung. *Biochemische Zeitschrift*, **49** 333-369.

[16] Richalet J. (1993). Industrial applications of model based predictive control. *Automatica, IFAC* **29**(5), 1251–1274.

[17] Stein R., Bucci V., Toussaint N.C., Buffie C.G., Rätsch G., Pamer E.G. et al. (2013). Ecological Modeling from Time-Series Inference: Insight into Dynamics and Stability of Intestinal Microbiota. *PLOS Computational Biology* **9**(12), 1–11.

[18] Wang Y. & Boyd S. (2010). Fast Model Predictive Control using Online Optimization. *Control Systems Technology, IEEE Transactions on,* **18**(2), 267–278.

[19] Wilson E. (2011). Force response of locust skeletal muscle. Southampton University, Ph.D. thesis.